

Morphology Control and Electroluminescence of ZnO Nanorod/GaN Heterojunctions Prepared Using Aqueous Solution

Sam-Dong Lee,[†] Yoon-Seok Kim,[‡] Min-Su Yi,[§] Jae-Young Choi,^{||} and Sang-Woo Kim*,[†]

School of Advanced Materials and System Engineering, Kumoh National Institute of Technology, Gumi, Gyeongbuk 730-701, Republic of Korea, Department of Electronics Science and Engineering, Kyoto University, Kyoto 615-8510, Japan, Department of Materials Science and Engineering, Kyungpook National University, Sangju, Gyeongbuk 742-711, Republic of Korea, and Multifunctional Device Group, Display Laboratory, Samsung Advanced Institute of Technology, Mt. 14-1, Nongseo, Yongin, Gyeonggi 446-712, Republic of Korea

Received: December 9, 2008; Revised Manuscript Received: February 15, 2009

We report on the morphology control and electroluminescence of well-aligned ZnO nanorod/p-GaN heterojunctions prepared by an aqueous solution route at low temperature (90 °C). We found that the density and size of the grown nanorods and microrods depended significantly on the ZnO seed density. Synchrotron X-ray scattering measurements showed an epitaxial relationship between the ZnO nanorods and the p-GaN thin film. ZnO nanorod/p-GaN heterojunction light-emitting diodes (LEDs) with an individual chip size of 300 × 300 μm² were fabricated. Room-temperature electroluminescence spectra in the visible range were obtained from the LED at forward bias voltage. This result indicates that such heterojunction LEDs fabricated from solution are a promising approach for realizing large-area light-emitting sources that have high external quantum efficiency.

1. Introduction

ZnO is a promising material for ultraviolet (UV) and white light-emitting diode (LED) applications, because of its large exciton binding energy of 60 meV relative to the thermal energy of 25 meV, as well as its large band gap of 3.37 eV at room temperature.^{1,2} In the past few years, the fabrication and characterization of one-dimensional (1D) ZnO nanostructures have been extensively investigated for their applications, such as LEDs,³ gas sensors,⁴ field emission devices,⁵ nanolasers,⁶ and photovoltaics.⁷ Despite many advances in 1D ZnO nanostructure research, the control of size, orientation, and density of 1D ZnO nanostructures remains an important issue in the progression toward efficient nanodevices.^{8–11}

Although there have been many efforts to realize ZnO p–n junction LEDs with high efficiency for commercial applications,¹² successful accomplishment of stable and highly conductive p-type ZnO is not available at the present stage. On the other hand, there have been several reports dealing with the observation of EL emission from ZnO thin film and nanorod heterojunctions with p-SrCu₂O₂ and p-GaN thin films.^{13–15} The ZnO nanorods were grown by metal organic chemical vapor deposition (MOCVD) for the realization of ZnO nanorod/p-GaN heterojunction LEDs.^{14,15} However, the MOCVD method generally involves high-temperature growth conditions, expensive and energy-consuming processes, and extremely limited growth environments. High-temperature processes seriously limit device applications and increase the thermal strain in the resulting nanostructures.

An alternative approach for synthesizing 1D ZnO nanostructures is the aqueous solution method. This has been widely

studied in view of its simplicity, low growth temperature, large-scale growth, flexible application, and mass productivity. Nevertheless, many challenges remain in order to realize uniformly distributed and well-aligned 1D ZnO nanostructure arrays with high crystallinity on a large scale.^{16,17} Detailed investigations of the morphology of 1D ZnO nanostructures during deposition in relation to the growth conditions in this process can provide information helpful to the control of 1D ZnO nanostructures.

We discuss here the morphology and density control of epitaxial ZnO nanorods on p-GaN thin films by manipulating a seed layer using an aqueous solution route at low temperature (90 °C). Electroluminescence (EL) from ZnO nanorod/p-GaN heterojunction LEDs at forward bias voltage is also studied. The EL emission suggests that the ZnO nanorods synthesized by this means have structural and optical properties suitable for application in 1D ZnO nanostructure-based LEDs.

2. Experimental Section

p-GaN templates were prepared by growing a 1-μm thick Mg-doped p-type GaN thin film on resistive undoped GaN on a *c*-plane sapphire substrate, in a 6 × 2 Thomas Swan CCS (close coupled showerhead) MOCVD system. The procedure for preparing p-type GaN on sapphire is as follows. A low-temperature GaN buffer layer was first deposited at 550 °C, and the temperature was then increased to 1030 °C. To ensure basic crystal quality, undoped GaN was grown to a thickness of 0.3 μm. p-type GaN was then grown to 1 μm thickness, using 3 μmol of Cp₂Mg as a p-type dopant, and carrier activation was then performed by rapid thermal annealing at 800 °C for 10 min. According to the Hall measurements, the hole concentration and mobility were 3 × 10¹⁷ cm^{−3} and 12 cm² V^{−1} s^{−1}. The ZnO seed layer on the p-GaN template was formed by dipping the template into 5 mM of zinc acetate [Zn(C₂H₃O₂)₂] dissolved in deionized (DI) water at 90 °C. To control the seed

* Corresponding author. E-mail address: kimsw@kumoh.ac.kr

[†] Kumoh National Institute of Technology.

[‡] Kyoto University.

[§] Kyungpook National University.

^{||} Samsung Advanced Institute of Technology.

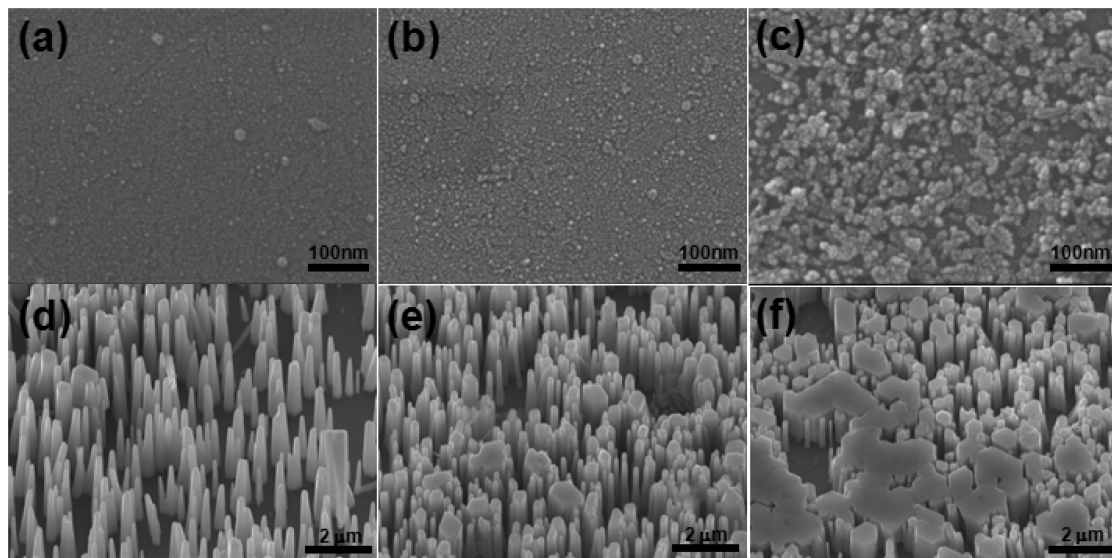


Figure 1. (a–c) FE-SEM images showing surface morphologies of ZnO seed layers as a function of dipping time and the number of dippings: (a) one dipping (for 5 min), (b) one dipping (for 20 min), and (c) four dippings (each for 20 min). (d–f) Tilting-view FE-SEM images of the ZnO nanorods grown using the seed layers shown in panels a–c.

layer, the dipping time was chosen to be 5–30 min and there were one to four dippings. The seed-coated samples were then annealed for 20 min at 100 °C before the main growth. ZnO nanorods on the nanosized ZnO-seed-coated p-GaN epilayer were grown in a mixture solution consisting of DI water, 25 mM of zinc nitrate hexahydrate $[Zn(NO_3)_2 \cdot 6H_2O]$, and 25 mM of hexamethylenetetramine $[C_6H_{12}N_4]$ (HMT) for 4 h at 90 °C, using the “dipping-and-holding” process.

Well-aligned ZnO nanorod/p-GaN heterojunction LEDs, with an individual chip size of $300 \times 300 \mu\text{m}^2$, were fabricated using a conventional photolithography technique. Plasma-enhanced chemical vapor deposition was used to fill the free space between each ZnO nanorod with a 500-nm-thick SiO_2 layer, to prevent electrical shorting and reduce the surface leakage current. We confirmed that the SiO_2 filling is more effective for reducing surface leakage current than photoresist filling. An increase in the surface leakage current of the LED would lead to EL emission under the reverse bias voltage and weak external quantum efficiency.¹⁴ Sputtering was used to deposit a 200-nm-thick indium–tin oxide (ITO) layer as a transparent conducting electrode on the top surface of the ZnO nanorods. E-beam evaporation was used to deposit Ti/Au (200 nm) and Ni/Au (200 nm) pad electrodes on the ITO transparent electrode and on p-GaN, respectively. To ensure Ohmic contacts to both layers, rapid thermal annealing was carried out.

Field-emission scanning electron microscopy (FE-SEM) was used to examine the morphology of the samples. The structural properties of the resulting ZnO nanorods were investigated by synchrotron X-ray scattering measurements carried out at beamline 5C2 at Pohang Light Source (PLS). The synchrotron X-ray was focused vertically by a mirror, and a double bounce Si (111) monochromator was used to monochromatize the X-ray to a wavelength of 1.239 Å. Transmission electron microscopy (TEM) was used to study the crystallinity of a single nanorod. The photoluminescence (PL) properties of two different samples (Mg-doped p-type GaN thin film and ZnO nanorod/p-GaN heterojunction) were investigated at room temperature. The EL spectra from the LED sample were obtained using an OL-770 spectrometer.

3. Results and Discussion

Figure 1a–c shows the FE-SEM images of the ZnO seed layers formed on p-GaN films by the dipping process, viewed as a function of the dipping time and iteration number. The ZnO seed density and size increased significantly as the dipping time and number of dippings increased. The increased size of the ZnO seed nanoparticles is due to the agglomeration of individual nanoparticles with small diameters to reduce the surface energy. The FE-SEM images of the resulting ZnO nanorods on the seed layers are shown in Figure 1d–f. ZnO nanorods and microrods with good vertical alignment were grown on the p-GaN thin films that had the different ZnO seed densities (Figure 1a–c) using the same nanorod growth conditions (stated in the Experimental Section). Vertical alignment of the ZnO nanorods and microrods is due to a preferred growth direction along the *c*-axis of ZnO, normal to the p-GaN surface.¹⁸ As shown in Figure 1, the density and size of ZnO seeds cause striking changes to the morphology and size of the resulting ZnO nanorods and microrods, indicating that the density and size of the ZnO nanorods depend strongly on those of the ZnO seeds.^{19,20}

Figure 2 is a schematic illustration showing the formation mechanism of ZnO nanorods and microrods with different seed densities and sizes. Preheat treatments of the seed layers before main growth may cause enhanced adhesion of seed nanoparticles to the p-GaN surface and generate an epitaxial relationship between the ZnO seed layer and the p-GaN due to the low lattice mismatch of ZnO to GaN. We therefore suggest that uniformly distributed ZnO seed nanoparticles with very small diameters, mainly below 5 nm (Figure 1a,b), lead to the formation of vertically aligned ZnO nanorods with relatively uniform diameters during main growth (Figure 1d,e). Conversely, more dippings lead to a nonuniform distribution of aggregated seed nanoparticles with larger diameters, as mentioned above, which results in the formation of microrods as well as nanorods during main growth. To clarify the formation mechanism of the microrods, we simply increased the main growth time from 4 to 6 h using the seed layer shown in Figure 1c. In the left of Figure 2d is an FE-SEM image showing closely packed

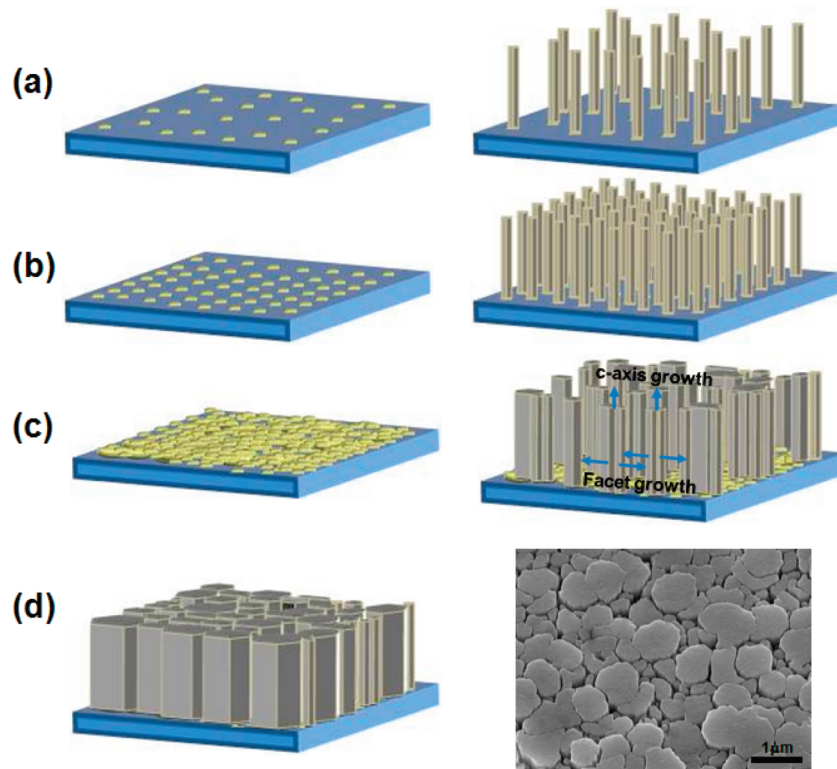


Figure 2. Schematic illustration of the formation mechanism of ZnO nanorods and microrods with differing seed densities and sizes. (a–c) Schematic images presenting the ZnO nanorod formation as a function of the ZnO seed density [(a) lower, (b) medium, and (c) higher]. On the right of part d is an FE-SEM image showing densely formed microrod arrays that resemble a thin film with many cracks during main growth for 6 h. On the left of part d is a schematic image showing facet growth of ZnO, resulting in microrod formation via the combination of individual nanorods.

microrod arrays that resemble a thin film with many cracks formed during the 6-h main growth time period. At the initial stage of ZnO growth, the growth of competing facets is determined by the fastest growth along the *c*-axis. However, the preferred *c*-axis growth gradually saturates at a critical growth time. From this time, the growth of facets proceeds, resulting in microrod formation by the combination of individual nanorods, as illustrated in the right side of Figure 2d.²¹

Figure 3a shows the powder diffraction profile for the ZnO nanorods shown in Figure 1e in synchrotron X-ray scattering measurements. The scan was taken along the surface normal direction, Q_z [$Q = 4\pi \sin(2\theta/2)/\lambda$], in reciprocal space. ZnO(0002) and GaN(0002) Bragg reflections, shown in Figure 3a, indicate that the ZnO nanorods and the GaN thin film were grown with $\langle 0001 \rangle$ orientation in the surface normal direction. Figure 3b shows the position of the nonspecular ZnO(10 $\bar{1}$ 2) reflection is in the same position of the nonspecular GaN(10 $\bar{1}$ 2) reflection, which shows that vertically well-aligned ZnO nanorods are in a perfect epitaxy relationship with the GaN thin film. The nonspecular ZnO(1012) reflection at every 60° position shows 6-fold symmetry, along with the GaN(10 $\bar{1}$ 2). Experimental observation of the epitaxial relationship between the ZnO nanorods and the GaN thin film indicates that the ZnO nanorods have promising structural properties in spite of the low growth temperature and solution synthesis approach.

To investigate the crystallinity of a single nanorod, we performed TEM measurements. Figure 4a shows a bright-field (BF) TEM image of a single ZnO nanorod. The high-resolution TEM (HRTEM) image shown in Figure 4b and a corresponding fast Fourier transformation (FFT) pattern (inset of Figure 4b), taken from the nanorod shown in Figure 4a, indicate that the lattice distance, measured from the lattice fringes along the

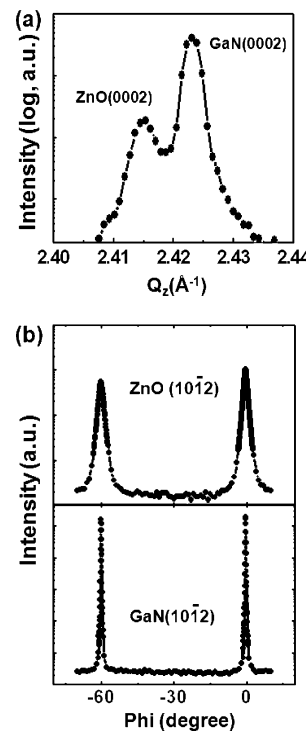


Figure 3. Synchrotron X-ray scattering measurements of ZnO/p-GaN heterostructures carried out at beamline 5C2 at PLS. (a) Bragg reflections of ZnO nanorods (0002) and the GaN thin film (0002) by powder X-ray diffraction measurement. (b) φ scans along the azimuth circles of ZnO(10 $\bar{1}$ 2) and GaN(10 $\bar{1}$ 2) nonspecular reflections.

growth axis direction of the ZnO nanorod, is 0.52 nm. This corresponds to the *c*-axis spacing of the (0002) atomic planes,

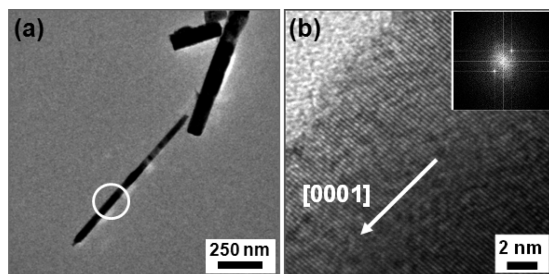


Figure 4. (a) BF TEM image of a single ZnO nanorod. (b) HRTEM image taken from the single nanorod (marked area in panel a). The inset shows the FFT pattern of the HRTEM image.

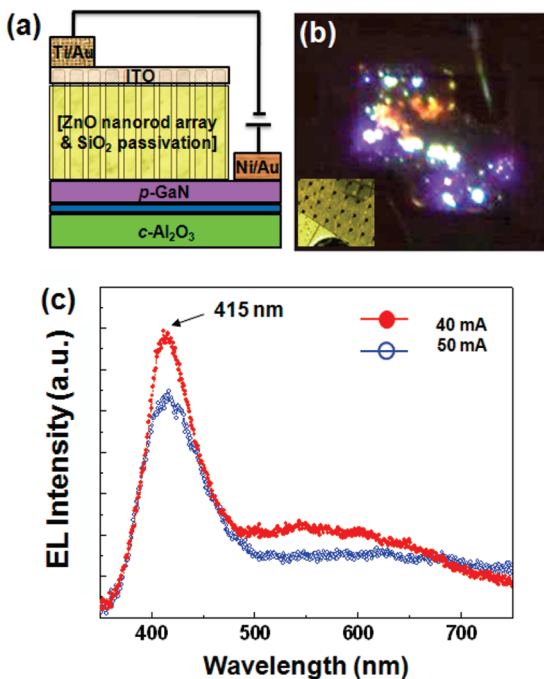


Figure 5. (a) Schematic illustration of the ZnO nanorod/p-GaN heterojunction LED. (b) Micrograph image showing EL emission from a nanorod/p-GaN heterojunction LED chip emitting violet, yellow, and white light at an injection current of 10 mA under forward bias. The inset of part b is an optical microscope image of ZnO nanorod/p-GaN heterojunction LED arrays with an individual $300 \times 300 \mu\text{m}^2$ chip. (c) EL spectra obtained from the ZnO nanorod/p-GaN heterojunction LED at higher injection currents of 40 and 50 mA under forward bias.

showing the preferred growth direction of [0001]. The anisotropic growth of the ZnO crystal along the [0001] direction is caused by the inherent polar properties along the *c*-axis. The FFT analysis along the [2110] zone axis of the ZnO nanorod demonstrates the single-crystalline nature of the nanorods grown along the [0001] direction, having a hexagonal crystal structure.

Figure 5a shows a schematic image of the ZnO nanorod/p-GaN heterojunction LED. The ZnO nanorods shown in Figure 1e were used in the LED fabrication. The nanosized heterojunctions are expected to have high external quantum efficiency as a result of their large surface areas that emit photons.²² Figure 5b shows a top-view image micrograph (captured using a CCD camera) of EL emission from a $300 \times 300 \mu\text{m}^2$ ZnO nanorod/p-GaN heterojunction LED chip: violet, yellow, and white light is emitted at an injection current of 10 mA under forward bias. The inset in Figure 5b shows an optical microscope image of the heterojunction LED arrays. Even though the violet, yellow, and white light emissions from the LED chip are clearly observed (Figure 5b), no EL spectrum could be obtained at this injection current of 10 mA. EL spectra from the ZnO nanorod/

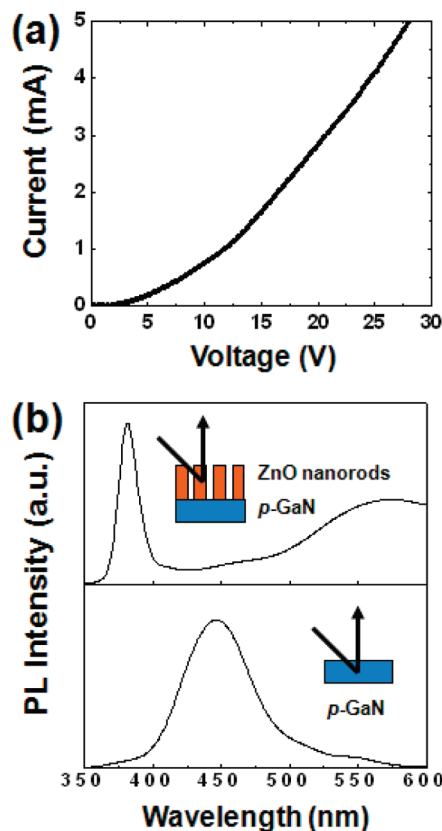


Figure 6. (a) *I*–*V* characteristics of the heterojunction LED under forward bias. (b) RT PL spectra from the Mg-doped p-type GaN thin film (lower) and the ZnO nanorod/p-GaN heterojunction (upper).

p-GaN heterojunction LED were observed at higher injection currents of 40 and 50 mA under forward bias. As shown in Figure 5c, the EL spectra show two clear emission bands, one centered on 415 nm and a broad emission band covering the range from 485 to 750 nm. Differences in the shape of the emission spectrum were not noticeable in the EL spectra between the injection currents of 40 and 50 mA. The EL spectra were obtained only under reverse bias in a previous report,¹⁴ but EL emission bands from our ZnO nanorod/p-GaN heterojunction LEDs under forward bias were clearly observed, despite the ZnO-nanorod growth at a low temperature of 90 °C in the chemical solution.

Figure 6a shows the current–voltage (*I*–*V*) characteristics of the heterojunction LED. However, it was very difficult to obtain reliable results on the emission output power of our LEDs in this work as a function of the applied forward voltage. As mentioned above, even though there was clear observation of the visible light emission from the LED chip (Figure 5b), no reliable EL spectrum was obtained at the injection current of 10 mA. The EL spectrum from the ZnO nanorod/p-GaN heterojunction LED fabricated in this work was obtained at the injection currents of 40 and 50 mA under the high forward biases of about 80 and 90 V, respectively. We believe that much larger forward voltage to achieve an EL emission spectrum compared with conventional LEDs is attributed to undoped ZnO nanorods with high resistivity and unstable metal contact between the ZnO nanorods and the transparent ITO electrode. In addition, the formation of point defects acting as carrier trapping and scattering centers is more favorable in nanorods grown using a solution method than in nanorods synthesized using other vacuum-based growth techniques such as MOCVD and thermal CVD accompanying high growth temperature.

To clarify the origin of the EL emission bands from the ZnO nanorod/p-GaN heterojunction LED, the PL properties of two samples of the Mg-doped p-type GaN thin film and the ZnO nanorod/p-GaN heterojunction sample were investigated at room temperature (Figure 6b). The PL spectrum of the Mg-doped p-type GaN thin film exhibited mainly a broad blue emission band centered on about 420 nm. The blue emission band is due to the band-to-acceptor transition that originates from deep Mg-related levels usually observed in Mg-doped p-GaN thin films.²³ The intense emission band centered on 380 nm in the PL spectrum^{12,24,25} obtained from the ZnO nanorod/p-GaN heterojunction sample is due to the free-exciton emission of ZnO. A broad emission band centered on about 570 nm was also observed, which may be due to the recombination of electrons at the conduction band with holes trapped in oxygen-related defects.²⁶ Considering a band diagram of the undoped ZnO/p-type GaN heterojunction,^{12,15} holes are expected to be injected from p-GaN into the ZnO nanorods under forward bias. Recombination of the holes and electrons therefore occurs in the ZnO nanorods.

Interestingly, the intense PL emission band centered on 380 nm was observed in the ZnO nanorod/p-GaN heterojunction. However, the EL emission bands centered on 415 nm dominated at 40 and 50 mA under forward bias, showing a large difference between PL and EL emission characteristics. In addition, the 415-nm EL emission band at 50 mA had a lower emission intensity than that at 40 mA. We propose that the large red-shift of EL emission relative to PL emission and the lower EL emission intensity at the higher injection current are due to excess hole injection from the p-GaN thin film into the ZnO nanorods at high injection current.¹⁵ The excess carriers cause thermal band gap narrowing²⁷ in the ZnO nanorods, resulting in an increase of nonradiative recombination as well as a red-shift of the emission band. In addition, an increase in the junction temperature with the rising injection current also needs to be considered for the red-shift of EL emission and degradation in the EL intensity.²⁸ ZnO nanostructures synthesized by the solution method generally contain a large number of point defects.²⁹ Moreover, surface states are strikingly generated by nanostructuring.³⁰ We therefore conclude that yellow and white EL emissions are due to transitions from various kinds of deep levels, formed by point defects or surface states, to the valence band in the ZnO region.

4. Conclusions

We have considered the control of the morphology and density and the electroluminescence of well-aligned ZnO nanorod/p-GaN heterojunctions, using a simple aqueous solution method of preparation at a low temperature of 90 °C. Uniformly distributed ZnO seed nanoparticles of smaller diameters led to the formation of vertically aligned ZnO nanorods with relatively uniform diameters during the main growth. More dippings led to a nonuniform distribution of agglomerated seed nanoparticles with larger diameters, resulting in the formation of microrods as well as nanorods during the main growth. ZnO nanorods have a perfect epitaxial relationship to the GaN thin film in the synchrotron X-ray scattering measurements. Strong EL spectra were obtained in the visible range from a size $300 \times 300 \mu\text{m}^2$ single chip ZnO nanorod/p-GaN heterojunction LED. We

believe that the results in this work are a significant step toward the realization of nanomaterial-based novel optical and electrical devices requiring low-temperature processes on a large scale.

Acknowledgment. This work was financially supported by the Korea Research Foundation Grant funded by the Korean Government (MOEHRD, Basic Research Promotion Fund) (KRF-2007-313-D00475) and by Samsung Advanced Institute of Technology. Synchrotron X-ray scattering experiments at PLS were supported in part by the Ministry of Education, Science and Technology (MEST) and POSTECH, South Korea.

References and Notes

- Huang, M. H.; Mao, S.; Feick, H.; Yan, H.; Wu, Y.; Kind, H.; Weber, E.; Russo, R.; Yang, P. *Science* **2001**, *292*, 1897.
- Alivov, Y. I.; Kalinina, E. V.; Cherenkov, A. E.; Loo, D. C.; Ataev, B. M.; Omaev, A. K.; Chukichev, M. V.; Bagnall, D. M. *Appl. Phys. Lett.* **2003**, *83*, 4719.
- Nadarajah, A.; Word, R. C.; Meiss, J.; Könenkamp, R. *Nano Lett.* **2008**, *8*, 534.
- Chang, S.-J.; Hsueh, T.-J.; Chen, I.-C.; Huang, B.-R. *Nanotechnology* **2008**, *19*, 175502.
- Wang, X.; Zhou, J.; Lao, C.; Song, J.; Xu, N.; Wang, Z. L. *Adv. Mater.* **2007**, *19*, 1627.
- Zhang, Y.; Russo, R. E.; Mao, S. S. *Appl. Phys. Lett.* **2005**, *87*, 043106.
- Law, M.; Greene, L. E.; Johnson, J. C.; Saykally, R.; Yang, P. *Nat. Mater.* **2005**, *4*, 455.
- Zhang, R.; Kumar, S.; Zou, S.; Kerr, L. L. *Cryst. Growth Des.* **2008**, *8*, 381.
- Alivisatos, A. P. *Science* **1996**, *271*, 933.
- Xia, Y.; Yang, P.; Sun, Y.; Wu, Y.; Mayers, B.; Gates, B.; Yin, Y.; Kim, F.; Yan, H. *Adv. Mater.* **2003**, *15*, 353.
- Geng, J.; Lu, D.; Zhu, J.; Chen, H. *J. Phys. Chem. B* **2006**, *110*, 13777.
- Hwang, D.-K.; Kang, S.-H.; Lim, J.-H.; Yang, E.-J.; Oh, J.-Y.; Yang, J.-H.; Park, S.-J. *Appl. Phys. Lett.* **2005**, *86*, 222101.
- Ohta, H.; Kawamura, K.; Orita, M.; Hirano, M.; Sarukura, N.; Hosono, H. *Appl. Phys. Lett.* **2000**, *77*, 475.
- Park, W. I.; Yi, G. C. *Adv. Mater.* **2004**, *16*, 87.
- Jeong, M.-C.; Oh, B.-Y.; Ham, M.-H.; Myoung, J.-M. *Appl. Phys. Lett.* **2006**, *88*, 202105.
- Peng, W.; Qu, S.; Cong, G.; Wang, Z. *Cryst. Growth Des.* **2006**, *6*, 1518.
- Weintraub, B.; Deng, Y.; Wang, Z. L. *J. Phys. Chem. C* **2007**, *111*, 10162.
- Pauporte, T.; Lincot, D.; Viana, B.; Pellé, F. *Appl. Phys. Lett.* **2006**, *89*, 233112.
- Song, J.; Lim, S. *J. Phys. Chem. C* **2007**, *111*, 596.
- Tak, Y.; Yong, K. *J. Phys. Chem. B* **2005**, *109*, 19263.
- Park, D. J.; Kim, D. C.; Lee, J. Y.; Cho, H. K. *Nanotechnology* **2007**, *18*, 395605.
- Jeong, M.-C.; Oh, B.-Y.; Ham, M.-H.; Lee, S.-W.; Myoung, J.-M. *Small* **2007**, *3*, 568.
- Smith, M.; Chen, G. D.; Lin, J. Y.; Jiang, H. X.; Salvador, A.; Sverdlov, B. N.; Botchkarey, A.; Morkoc, H.; Goldenberg, B. *Appl. Phys. Lett.* **1996**, *68*, 1883.
- Zu, P.; Tang, Z. K.; Wong, G. K. L.; Kawasaki, M.; Ohtomo, A.; Tamura, K.; Koinuma, H.; Segawa, Y. *Solid State Commun.* **1997**, *103*, 459.
- Makino, T.; Tuan, N. T.; Segawa, Y.; Chia, C. H.; Kawasaki, M.; Ohtomo, A.; Tamura, K.; Koinuma, H. *Appl. Phys. Lett.* **2000**, *76*, 3549.
- Studenikin, S. A.; Cocivera, M. *J. Appl. Phys.* **2002**, *91*, 5060.
- Mukai, T.; Yamada, M.; Nakamura, S. *Jpn. J. Appl. Phys.* **1998**, *37*, L1358.
- Cho, J.; Sone, C.; Park, Y.; Yoon, E. *Phys. Status. Solidi A* **2005**, *202*, 1869.
- Govender, K.; Boyle, D. S.; Brien, P. O.; Blinks, D.; West, D.; Coleman, D. *Adv. Mater.* **2002**, *14*, 1221.
- Shalish, I.; Temkin, H.; Narayananmurti, V. *Phys. Rev. B* **2004**, *69*, 245401.